Modelling of charge injection by multi-photon absorption in GaN-on-Si HEMTs for SEE testing

C. Ngom, Vincent Pouget, M. Zerarka, F. Coccetti, O. Crepel, A. Touboul, M. Matmat

Modelling of Charge Injection by Multi-Photon Absorption in GaN-on-Si HEMTs for SEE Testing

C. Ngom[a,b,*], V. Pouget[b], M. Zerarka[a], F. Coccetti[a], O. Crepel[c], A. Touboul[c], M. Matmat[a]

[a] *IRT Saint-Exupery,Toulouse, France*
[b] *IES, Université de Montpellier, CNRS, Montpellier, France*
[c] *Airbus,Toulouse, France*

Abstract

This paper presents the numerical evaluation of different multiphotonic absorption mechanisms to be used for backside laser testing of single-event effects in GaN-on-Si HEMTs. The optical transmission through the complete stack of layers of three commercial references is calculated. Experimental results illustrating the possibility to use three-photon absorption for charge injection in the GaN layer are presented. The possible contribution of higher-order optical absorption in the buffer layers is discussed.

1. Introduction

Gallium Nitride (GaN) is one of the most promising Wide Band Gap materials [1] thanks to its excellent physical properties. GaN devices are good alternatives to Si technologies as they present low ON-state resistance (RON) and high breakdown voltage [1] with respect to Si devices. GaN technologies are compatible with high-voltage operation thanks to the wide energy gap and the high critical electric field [2] with a reduction of the power losses.

Single event effects (SEEs) are one of the main causes of devices failures in space and aeronautic power applications. The conventional technique for SEE characterization consists in using broad particle beams such as heavy ions. Laser testing is a complementary technique, which can provide interesting additional information on the failure mechanisms of the devices. It has been well demonstrated on Si technologies including power devices [3] but needs to be validated on commercial GaN devices. There are a few papers addressing SEE on research GaN HEMTs using single-photon absorption with UV laser [4] and two-photon absorption with visible light [5] through the device front-side. For commercial devices, the laser beam is not able to pass through the front-side metal layers, which prevents the use of the front-side approach. Thus, there is a strong interest for developing the backside laser testing approach on GaN COTS, which consist in focusing the beam through the backside layer stack to inject charge in the active layer of the device.

In this paper, we present an analytical modelling of the backside laser testing technique performed on commercial GaN-on-Si HEMTs. This study allows to complete our previous experimental work [6] with supplementary modelling. The objective of the modelling is to identify the absorption mechanisms that allows generating charges in GaN HEMT and estimate the fraction of the amount of charge that reach the active layers. First, the laser energy required to generate charge in a block of GaN at wavelengths in the visible and near-infrared domains is estimated.

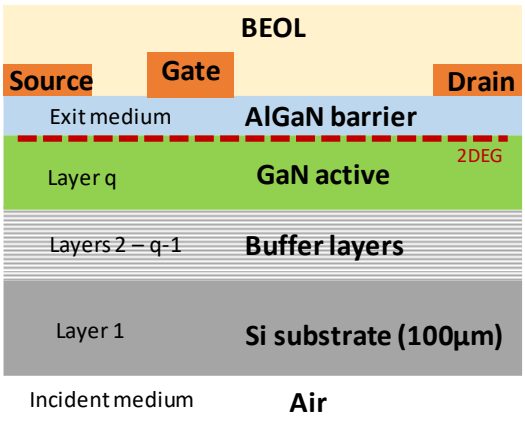

Fig. 1. Structure of the GaN HEMTs under study.

* Corresponding author. catherine.ngom@ies.univ-montp2.fr

Table 1
Layer stack composition and thickness of the three references

Ref A		Ref B		Ref C	
Material	Thickness	Material	Thickness	Material	Thickness
GaN	0.9 µm	GaN	2 µm	GaN	1.8 µm
				$Al_{0.25}Ga_{0.75}N$/GaN superlattice	0.8 µm
$Al_{0.06}Ga_{0.94}N$	0.5 µm	AlN/GaN superlattice	2 µm		
$Al_{0.2}Ga_{0.8}N$	0.5 µm			$Al_{0.1}Ga_{0.9}N$	0.6 µm
$Al_{0.3}Ga_{0.7}N$	0.4 µm	$Al_{0.06}Ga_{0.94}N$	0.2 µm	$Al_{0.2}Ga_{0.8}N$	0.6 µm
$Al_{0.5}Ga_{0.5}N$	0.2 µm			$Al_{0.4}Ga_{0.6}N$	0.3 µm
				$Al_{0.7}Ga_{0.3}N$	0.1 µm
AlN	0.3 µm	AlN	0.2 µm	AlN	0.2 µm

Then, the transmittance of the backside layer stack of the HEMT is calculated. Experimental results are provided.

2. Test vehicle

The devices of interest for this study are named ref A, ref B and ref C. Fig. 1. shows the common backside structure of the devices and their respective detailed composition is presented in Table 1. The Al content of the AlGaN barrier layer is 27%. The Si substrate is considered as undoped and its post-preparation thickness is fixed at 100µm for the three devices of interest.

3. Theoretical models

The photon wavelengths simulated are comprised in the range 345-1725 nm. The photon–semiconductor interaction is based on a photoelectric mechanism that can be either linear, this is the Single-photon absorption (SPA) or non-linear: Two-photon absorption (2PA), Three-photon absorption (3PA), Four-photon absorption (4PA) and Five-photon absorption (5PA).

3.1. Multiphoton interband absorption coefficient

Among the input parameters of the model, there is the absorption coefficient corresponding to the studied mechanism. The absorption coefficient β_{NPA} governs the N-photon absorption mechanism. The theoretical model below from [7] allows to calculate the inter-band multi-photon absorption coefficient for direct-gap materials.

$$\beta_{NPA}(\hbar\omega) = C_N F_N \left(\frac{N\hbar\omega}{E_g}\right) \frac{\hbar^{N-1} P^{2N-3}}{n^N {E_g}^{4N-5}} \qquad (1)$$

where n is the refractive index, E_g the bandgap energy and the Kane parameter defined as $P = \hbar\sqrt{E_p/2m_0}$ with E_p the Kane energy and m_0 the electron mass. C_N is a dimensionless factor, as well as F_N which is a function of $\frac{N\hbar\omega}{E_g}$ which will thus give the dependency of the absorption coefficient with respect to the wavelength. They are defined according to whether N is even or odd.

Other factors not taken into account in the equation must be added to obtain an exact amplitude of the absorption coefficient [7]. For 2PA mechanism, the factors were estimated to 12 and 1/5, which are the adjustment factor generally used in the literature. All of these additional factors tend to increase the amplitude of the absorption coefficient β_{NPA}.

3.2. Thin layers stack transmittance

Considering a beam that propagates through a superposition of layers with complex refractive index $\tilde{n}_i$ and thickness d_i, the transmittance can be obtained with a matrix-based calculation. The approach consists of using the characteristic matrix of each layer [8] for beam normal incidence:

$$M_i = \begin{bmatrix} \cos\varphi_i & (i/\tilde{n}_i)\sin\varphi_i \\ i\tilde{n}_i \sin\varphi_i & \cos\varphi_i \end{bmatrix} \qquad (2)$$

where $\varphi_i = \frac{2\pi}{\lambda}\tilde{n}_i d_i$ is the phase shift inside the layer.

The overall characteristic matrix of the layer stack is:

$$M = \begin{bmatrix} m_{11} & m_{12} \\ m_{21} & m_{22} \end{bmatrix} = \prod_{i=q}^{1} M_i \qquad (3)$$

The amplitude of transmission coefficient is given by:

$$t = \frac{2\eta_{inc}}{\eta_{inc} m_{11} + \eta_{ex} m_{22} + \eta_{inc}\eta_{ex} m_{12} + m_{21}} \qquad (4)$$

where η_{inc} and η_{ex} are pseudo-indices of incident and exit mediums.

The overall transmittance of the stack is given by $T = (Re\{\tilde{n}_{ex}\}/Re\{\tilde{n}_{inc}\})\, tt^*$ where * is the complex conjugate and $Re\{\tilde{n}_{ex,inc}\}$ the real part of the refractive index.

4. Modelling methodology and results

To identify the different absorption mechanisms (SPA, 2PA, 3PA, etc.) that can be used for laser testing and the optical parameters to be used, a calculation tool in C based on the above models has been implemented. The approach was to divide the modelling into several levels. The level 1 estimates the order of magnitude of the required laser energies in GaN material. The level 2.1 calculates the total transmittance of the backside layer stack of GaN HEMTs using only layer attenuation due to linear absorption and interface reflections. The level 2.2 takes into account the layers interferences in the transmittance calculation if a plane wave is used. The level 2.3 takes into account the convergence of the Gaussian beam by combining level 2.1 and 2.2. An additional level that takes into account the non-linear propagation would provide a more accurate estimation of the transmittance but it is left for future works.

4.1. Level 1: Estimation of the laser energies in GaN material

We compare the order of magnitude of the required laser energies for charge injection in Si and GaN materials. For a given laser energy, the charge distribution amplitude in Silicon is calculated for the SPA mechanism. Then, the laser energy required to obtain the same charge distribution amplitude in GaN is calculated using the SPA, 2PA, 3PA, 4PA and 5PA absorption mechanisms following this equation:

$$E_L = \frac{\pi^{3/2}{\omega_0}^2\tau}{2}\left(\frac{NE_\gamma N_{0_{SPA}}}{\beta_{NPA}\sqrt{\pi}\tau}\right)^{1/N} \qquad (5)$$

where $E\gamma$ is the photon energy, $N_{0_{SPA}}$ is the reference charge distribution amplitude in silicon, ω_0 is the waist of the Gaussian beam and τ is the pulse duration.

4.1.1. N-photon absorption coefficient

The absorption coefficients β_{2PA}, β_{3P}A, and β_{4PA} calculated with Eq. 1 are presented in Fig. 2. The 2PA coefficients is consistent with the calculation results of Sun et al. [9] and Chen et al. [10] in terms of absorption coefficient and wavelength dependency. To obtain an agreement in terms of amplitude, the correction factors 12 and 1/5 were introduced for the 2PA as did Sun et al. and Chen et al. For higher order absorption coefficients β_{3PA} to β_{5PA}, the correction factors remain unknown, thus in our calculations they are considered to be equal to 1.

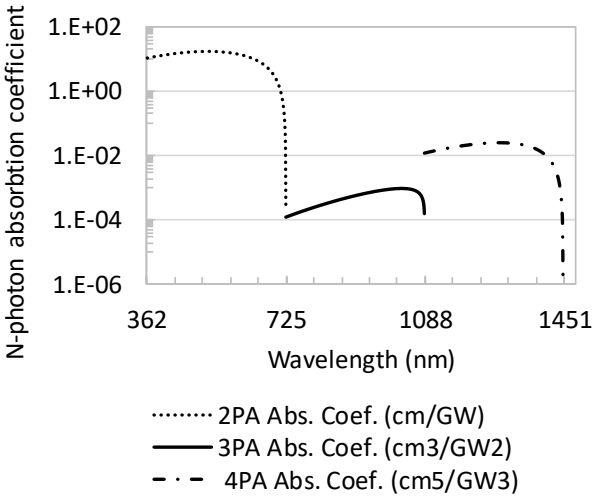

Fig. 2. N-photon absorption coefficient as a function of normalized wavelength in GaN.

4.1.2. Comparison of required laser energy for Si and GaN material

For the SPA and 2PA mechanisms, the laser energy is calculated for a pulse duration of 30ps and 0.32ps respectively. For the 3PA, 4PA and 5PA mechanisms, the pulse durations used are 0.32ps and 0.1ps. The beam waist is fixed to 1µm.

For Silicon and GaN, the SPA absorption coefficients used for the calculation are provided by databases in the literature. The absorption mechanisms with even N are more efficient because the required energy is lower than those with odd N as we can see in Fig. 3. The 3PA mechanism seems to be

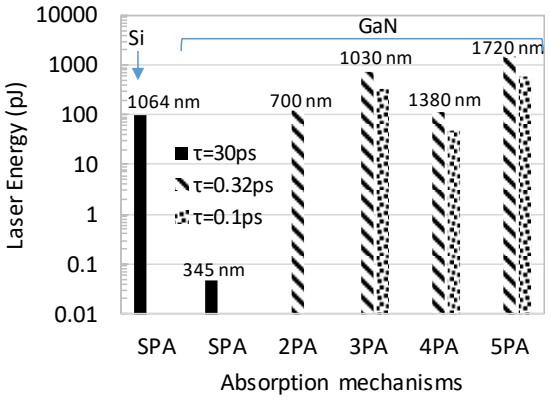

Fig. 3. Required laser energy at a given wavelength for each absorption mechanism.

possible for GaN at 1030 nm, which is close to wavelengths commonly used for SPA in Si (1064 nm). The 4PA mechanism at 1380 nm is more efficient than 3PA but laser source at this wavelength is more difficult to obtain in femtosecond regime.

4.2. Level 2.1: Calculation of the total backside layer stack transmittance of GaN HEMTs

For backside testing approach on GaN HEMT, the beam passes through the substrate and buffer layers. During its propagation through the different layers, the beam is attenuated and part of the flux is reflected at each interface.

The transmittance calculation of this stack allows to estimate the proportion of the beam intensity at the level of the GaN active layer.

The transmittance calculation takes into account only the attenuation due to the linear absorption in each layer and the transmittance of the different interfaces. It does not take into account attenuation due to multi-photon absorption, Kerr effect, etc.

The calculated transmittance in Fig. 4. is dominated by the absorption in the Si substrate and the contribution of each interface transmittance.

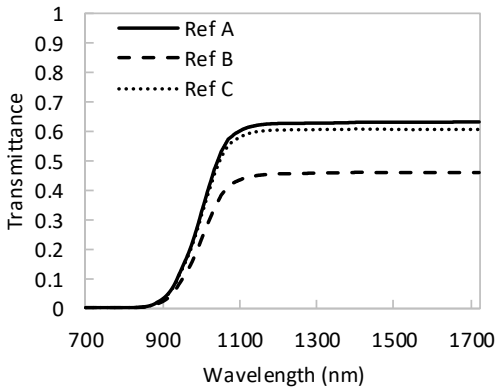

Fig. 4. Backside layer stack transmittance as a function of wavelength with Level 2.1 modelling for ref A, ref B and ref C.

4.3. Level 2.2: Considering the interferences in the transmittance calculation

The reflected part of the laser beam on each interface can generate interferences. To take into account these interferences, the matrix-based model is applied. In this part, the convergence of the beam is not taken into account yet. The beam inside the layer stack is assumed to be a plane wave.

We can see in Fig. 5. that interferences introduce strong oscillations in the transmittance but this result is not realistic for our case studies. This model is only valid for plane waves; hence, for Gaussian beam it is necessary to take into account the convergence of the beam to obtain realistic results.

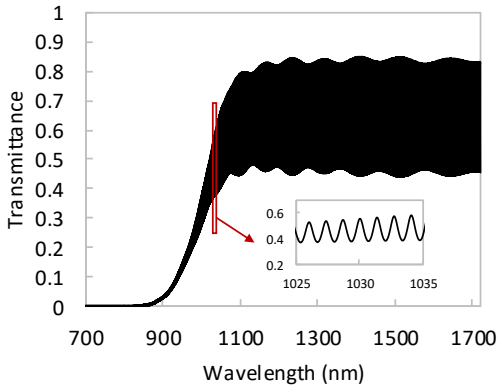

Fig. 5. Backside layer stack transmittance as a function of wavelength with Level 2.2 modelling for ref C.

4.4. Level 2.3: Considering the beam convergence in the transmittance calculation

To take into account the beam convergence, an additional step in the calculation is necessary. The composite Rayleigh length related to the beam convergence is calculated to know the DUT layers where the beam can be considered as plane wave. The beam waist is supposed to be at the AlGaN/GaN interface. Thus, if the sum of the buffer and the GaN active layers thickness is lower than the composite Rayleigh length, we can consider the beam as a plane wave and then take into account interferences in buffer and GaN layers. Moreover, if the substrate thickness is higher than the composite Rayleigh length, we can consider that no interference occurs in the substrate. For the three devices of interest, the composite Rayleigh length calculated is about 9 µm, which mean the considerations above can be applied. The beam width evolution inside the GaN HEMT is presented in Fig. 6. We can see the refraction change

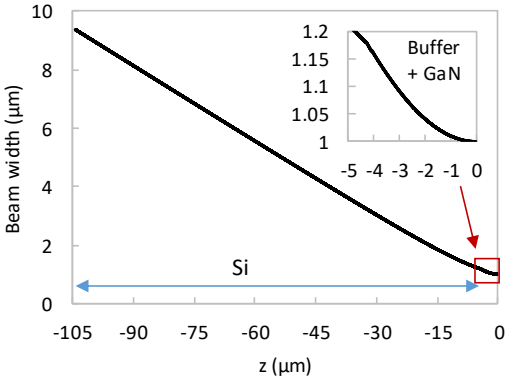

Fig. 6. Laser beam width through backside layer stack for ref C.

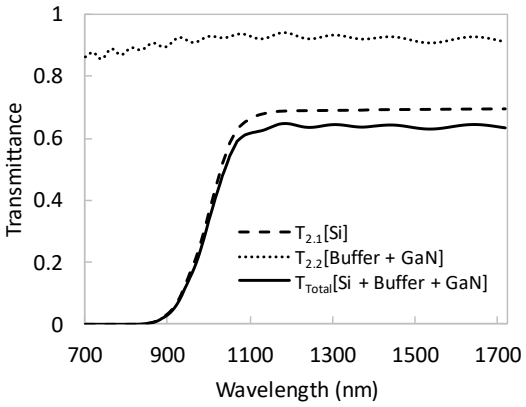

Fig. 7. Backside layer stack transmittance as a function of wavelength with Level 2.3 modelling for ref A.

at the interface between the substrate and the buffer layer. The refractive indices of the different layers of the buffer and the GaN active layer are close. Thus, the change is not significant.

Fig. 7. shows the intermediate calculations of the backside transmittance. The substrate transmittance is calculated with Level 2.1 modelling which doesn't take into account interferences. The transmittance of the set buffer + GaN active is obtain withLevel 2.2 modelling which consider interferences. The total backside transmittance is obtained by multiplying the transmittance of the substrate and the set buffer + GaN active. We can see the attenuation is mainly caused by the Si substrate layer.

The results in Fig. 8. shows that the transmittance of the three references are similar and is consistent with low impact of the buffer and GaN layers. SPA and 2PA mechanisms in GaN are not possible because of the attenuation in the Si substrate. The 3PA mechanism seems possible at 1030 nm with a transmittance of 46% for a Si substrate thickness less than or equal to 100µm. The 4PA and 5PA

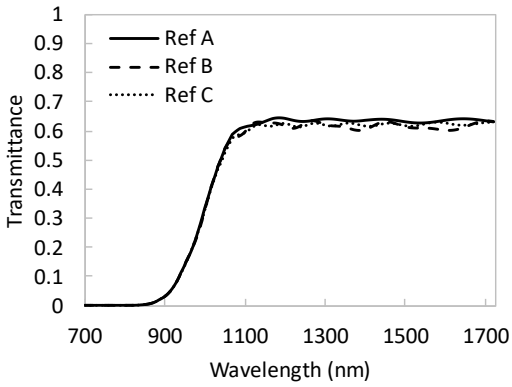

Fig. 8. Backside layer stack transmittance as a function of wavelength with Level 2.3 modelling for ref A, ref B and ref C.

Table 2
Layer bandgap and NPA absorption coefficient at 1030 nm for ref A

Material	Eg (eV)	λg (nm)	N	N.λg (nm)	Absorption coefficient
GaN	3.42	363	3	1089	10^{-3} cm^3/GW^2
$Al_{0.06}Ga_{0.94}N$	3.59	345	3	1035	$4.1\cdot10^{-3}$ cm^3/GW^2
$Al_{0.2}Ga_{0.8}N$	3.98	312	4	1248	$4.5\cdot10^{-3}$ cm^5/GW^3
$Al_{0.3}Ga_{0.7}N$	4.25	291	4	1164	$2.5\cdot10^{-3}$ cm^5/GW^3
$Al_{0.5}Ga_{0.5}N$	4.81	258	4	1032	$2.2\cdot10^{-6}$ cm^5/GW^3
AlN	6.20	200	> 5		
Si	1.12	1108	1	1108	30 cm^{-1}

mechanisms also seem possible with a transmittance of 60%. For the reasons mentioned in section 4.1.2, the 3PA approach is preferred.

4.5. Longitudinal profile for Ref A

Table 2 provides the bandgap energy and the lower absorption mechanism order possible in each layer at 1030 nm for ref A. The equivalent wavelength to the bandgap energy *Eg* corresponds to *λg*. At 1030 nm, charge is generated simultaneously in the different layers. The NPA mechanism in each layer is

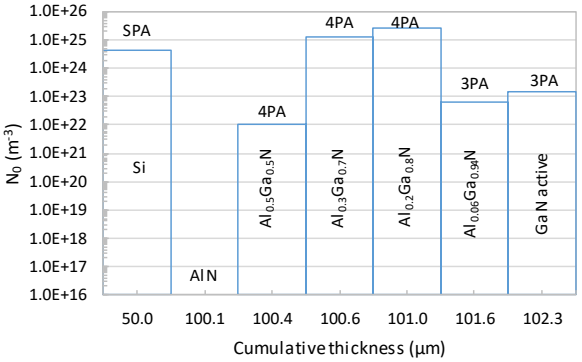

Fig. 9. Charge distribution amplitude in each layer for ref A.

possible with $N{\cdot}\lambda g$ higher than 1030 nm. For ref A, charge in GaN active layer is mostly generated via 3PA while in AlGaN buffer with Al content higher than 7% the charge is mostly generated via 4PA. Note that in each layer higher orders NPA also contribute to the charge generation.

Fig. 9. shows the estimation of the charge distribution amplitude N_0 generated by the lower possible NPA mechanism in each layer. This calculation does not take into account the attenuation due to the non-linear absorption in the beam propagation. The charge induced in buffer is relatively important compared to that injected in GaN active layer.

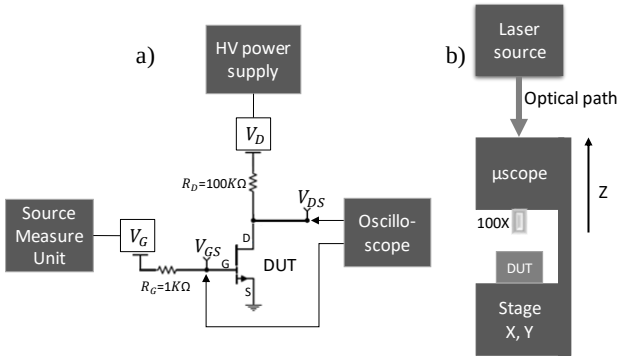

Fig. 10. Experimental setup: a) Electrical circuit; b) Laser bench.

These results obtained without considering the non-linear effects are a first step in the modelling of the laser interaction with GaN HEMT. Taking into account the beam depletion due to non-linear absorption of the buffer layers, and the Kerr and Plasma effects would provide more accurate results.

5. Experimental results

We tested commercial power GaN HEMT with a breakdown voltage of 650V. Experiments were performed at the laser facility of IES, University of Montpellier. The electrical circuit of the test bench and the experimental setup is presented in Fig. 10. The laser source wavelength is 1030 nm. The laser pulse duration is 320 fs at the laser output. The beam is focused using a 100X objective lens down to a knife-edge measured spot size of 1.0 µm. A 100 kΩ drain resistance and 1 kΩ gate resistance are used to limit the currents and to allow the observation of voltage transients. The source and the substrate contacts are connected to the ground.

Transients with amplitude of few mV and duration of few tens of µs have been observed on the gate channel as we can see in Fig. 11. Transients were also observed on the drain signal but were not exploited due to excessive noise from the power supplies. This confirm the possibility to inject charge

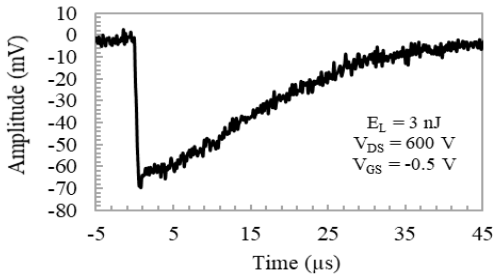

Fig. 11. Transients captured on the gate channel of the oscilloscope.

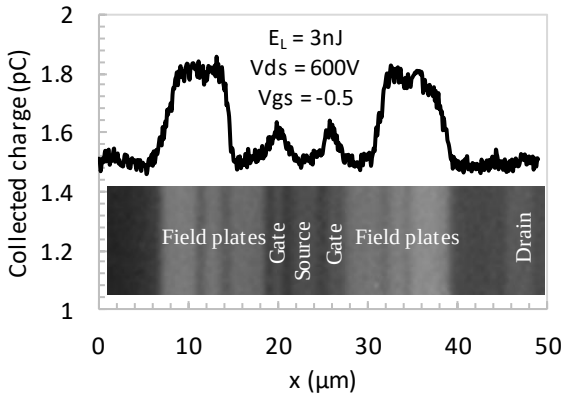

Fig. 12. Transients collected charge over the structure at laser energy of 6 nJ on Ref C.

in GaN HEMT. However, we demonstrated in [6] that the charge associated with the transient is dominated by SPA pair generation in the Silicon substrate. The contribution of the non-linear absorption in the GaN active and buffer layers needs to be further investigated.

Fig. 2. presents a mapping of the transient collected charge across the "fingers" of the device for ref C at laser energy of 6 nJ, V_{DS} = 600 V and V_{GS} = -0.5 V. We can observe that the collected charge depends on the laser spot position along the device. The maximum signal is observed near the gate contacts and the field plates. This strong contrast between the different regions shows the possibility to identify the most sensitive zones of the device.

6. Conclusion

We have presented an analytical modelling of the backside laser testing on GaN HEMTs. The estimated laser pulse energy required to generate charge in active layers seems reasonable using wavelength compatible with 3PA in GaN. Charge injection in the buffer and substrate layers has been also modeled. The consideration of the non-linear absorption in the beam attenuation and the Kerr and Plasma effects may be necessary to further improve the modelling of the charge generation with femtosecond pulse durations in these devices. Experimental results confirm the possibility of generating Single Event Transients using backside laser testing on commercial GaN power HEMTs.

References

[1] F. Roccaforte, P. Fiorenza, G. Greco, R. Lo Nigro, F. Giannazzo, F. Iucolano, and M. Saggio, "Emerging trends in wide band gap semiconductors (SiC and GaN) technology

for power devices," *Microelectron. Eng.*, vol. 187–188, pp. 66–77, Feb. 2018.

[2] M. Zerarka and O. Crepel, "Radiation robustness of normally-off GaN/HEMT power transistors (COTS)," *Microelectron. Reliab.*, vol. 88–90, pp. 984–991, Sep. 2018.

[3] S. P. Buchner, F. Miller, V. Pouget, and D. P. McMorrow, "Pulsed-Laser Testing for Single-Event Effects Investigations," *IEEE Trans. Nucl. Sci.*, vol. 60, no. 3, pp. 1852–1875, Jun. 2013.

[4] A. Khachatrian, N. J. Roche, S. P. Buchner, A. D. Koehler, J. D. Greenlee, T. J. Anderson, J. H. Warner, and D. McMorrow, "Spatial Mapping of Pristine and Irradiated AlGaN/GaN HEMTs With UV Single-Photon Absorption Single-Event Transient Technique," *IEEE Trans. Nucl. Sci.*, vol. 63, no. 4, pp. 1995–2001, Aug. 2016.

[5] A. Khachatrian, N. J. H. Roche, S. Buchner, A. D. Koehler, T. J. Anderson, V. Ferlet-Cavrois, M. Muschitiello, D. McMorrow, B. Weaver, and K. D. Hobart, "A Comparison of Single-Event Transients in Pristine and Irradiated Al0.3Ga0.7N/GaN HEMTs using Two-Photon Absorption and Heavy Ions," *IEEE Trans. Nucl. Sci.*, vol. 62, no. 6, pp. 2743–2751, Dec. 2015.

[6] C. Ngom, V. Pouget, M. Zerarka, F. Coccetti, A. Touboul, M. Matmat, O. Crepel, S. Jonathas, and G. Bascoul, "Backside Laser Testing of Single-Event Effects in GaN-on-Si Power HEMTs," *IEEE Trans. Nucl. Sci.*, 2021.

[7] B. S. Wherrett, "Scaling rules for multiphoton interband absorption in semiconductors," *J. Opt. Soc. Am. B*, vol. 1, no. 1, pp. 67–72, Mar. 1984.

[8] S. Larouche and L. Martinu, "OpenFilters: open-source software for the design, optimization, and synthesis of optical filters," *Appl. Opt.*, vol. 47, no. 13, pp. 219–230, 2008.

[9] C. K. Sun, J. C. Liang, J. C. Wang, F. J. Kao, S. Keller, M. P. Mack, U. Mishra, and S. P. DenBaars, "Two-photon absorption study of GaN," *Appl. Phys. Lett.*, vol. 76, no. 4, pp. 439–441, 2000.

[10] H. Chen, X. Huang, H. Fu, Z. Lu, X. Zhang, J. A. Montes, and Y. Zhao, "Characterizations of nonlinear optical properties on GaN crystals in polar, nonpolar, and semipolar orientations," *Appl. Phys. Lett.*, vol. 110, no. 181110, pp. 1–5, 2017.